Available online at www.sciencedirect.com

ScienceDirect

www.elsevier.com/locate/jes

JES JOURNAL OF ENVIRONMENTAL SCIENCES

www.jesc.ac.cn

Potential acute effects of suspended aluminum nitride (AlN) nanoparticles on soluble microbial products (SMP) of activated sludge

Lijie Zhou[1,2], *Weiqin Zhuang*[3], *Xin Wang*[2], *Ke Yu*[4], *Shufang Yang*[5], *Siqing Xia*[2,*]

1. *State Environmental Protection Key Laboratory of Drinking Water Source Management and Technology, Shenzhen Key Laboratory of Drinking Water Source Safety Control, Shenzhen Key Laboratory of Emerging Contaminants Detection & Control in Water Environment, Shenzhen Academy of Environmental Sciences, Shenzhen 518001, China*
2. *State Key Laboratory of Pollution Control and Resource Reuse, College of Environmental Science and Engineering, Tongji University, 1239 Siping Road, Shanghai 200092, China*
3. *Department of Civil and Environmental Engineering, University of Auckland, Auckland 1142, New Zealand*
4. *School of Environment and Energy, Peking University Shenzhen Graduate School, Shenzhen 518055, China*
5. *Shenzhen Municipal Design & Research Institute Co., Ltd, 3007 West Sungang Road, Shenzhen 518029, China*

ARTICLE INFO

Article history:
Received 21 October 2016
Revised 4 February 2017
Accepted 6 February 2017
Available online 14 February 2017

Keywords:
Aluminum nitride nanoparticles
Topic:
Soluble microbial products (SMP)
Activated sludge
Bacterial viability

ABSTRACT

The study aims to identify the potential acute effects of suspended aluminum nitride (AlN) nanoparticles (NPs) on soluble microbial products (SMP) of activated sludge. Cultured activated sludge loaded with 1, 10, 50, 100, 150 and 200 mg/L of AlN NPs were carried out in this study. As results showed, AlN NPs had a highly inverse proportionality to bacterial dehydrogenase and OUR, indicating its direct toxicity to the activated sludge viability. The toxicity of AlN NPs was mainly due to the nano-scale of AlN NPs. In SMP, AlN NPs led to the decrease of polysaccharide and humic compounds, but had slight effects on protein. The decrease of tryptophan-like substances in SMP indicated the inhibition of AlN NPs on the bacterial metabolism. Additionally, AlN NPs reduced obviously the molecular weight of SMP, which might be due to the nano-scale of AlN.

Introduction

A variety of engineered nanoparticles (NPs) is now widely used in commodities, pharmaceutics, cosmetics, biomedical products, and industries (Lee et al., 2015; Shaalan et al., 2016). It was reported that the worldwide consumption of NPs was nearly 220,000 metric tons in 2014 and kept an annual growth rate of 21.1% (Vale et al., 2016). As a result, NPs is increasingly released into the environment, particularly wastewater treatment plants (WWTPs) (Ma et al., 2016). Kiser et al. (2009) reported that raw sewage contained 100 to nearly 3000 μg TiO_2 NPs/L. The potential effects of NPs, especially TiO_2 NPs, Ag NPs, ZnO NPs, CuO NPs, *etc.*, on the ecosystem and environment has attracted great concerns (Lee et al., 2011; Liu et al., 2016; Nel et al., 2006). Due to the wurtzite structure of aluminum nitride (AlN) NPs, consisting of two

* *Corresponding author.*
E-mail address: siqingxia@gmail.com (S. Xia).

http://dx.doi.org/10.1016/j.jes.2017.02.001
1001-0742/

interpenetrating hexagonal closely-packed sublattices, AlN NPs exhibits many useful properties and has a wide application, such as electronic substrates, military, steel and semiconductor manufacturing, *etc.* (Lerner et al., 2016). However, though AlN NPs has been promoted to the manufacture process, the potential acute effects of AlN NPs on the environment, especially the wastewater treatment system, are unknown and ignored.

Soluble microbial products (SMP) has been defined as the pool of organic compounds that are released into aqua from substrate metabolism (usually with biomass growth) and biomass decay (Kunacheva and Stuckey, 2014). It is reported that SMP might reduce the pollutant removal efficiency of the biological processes and the quality of effluent, and even cause possible environmental hazard to the receiving water (Kunacheva and Stuckey, 2014; Xie et al., 2013). Therefore, lots of attentions have recently been paid to the characteristics of SMP in biological systems (Holakoo et al., 2006; Ni and Yu, 2012; Xie et al., 2013; Zhou et al., 2014). In addition, SMP has the strongest relationship with membrane fouling (Aslam et al., 2017; Deng et al., 2016; Jo et al., 2016; Wang et al., 2013). SMP could be readily deposited and adsorbed on and/or into the membrane owing to the permeation drag and higher Brownian diffusion (Deng et al., 2016). SMP with macromolecular character constituted the major soluble organic substances, encouraging the membrane pore blocking and the formation of gel layer and cake layer (Lin et al., 2014; Zhou et al., 2012). Fraction over 100 kDa in hydrophilic substances of SMP, mainly consisting of the polysaccharide-like substances, also engendered severe flux decline and pore blocking, and further size exclusion of SMP was concluded as the key role in irreversible fouling of hydrophilic substances (Shen et al., 2010, 2012). It was also reported that higher production of SMP implied the predominance of the pore blocking (Campo et al., 2016, 2017). Consequently, SMP was also considered as the key role in membrane fouling and attracted lots of interest in the area of wastewater treatment with membrane. The constituent, molecular weight (MW) and chelation of SMP are considered as its major characteristics. SMP is reported as the complex organic substance containing proteins, polysaccharide, humic acids, lipids, *etc.* (Ni and Yu, 2012). It is evident that SMP plays a significant role in the chelation for the metal ion removal in biological wastewater treatment (Holakoo et al., 2006). Although many studies concerned the characteristics of SMP, the potential acute effects of suspended AlN NPs, as a potential pollutant, on SMP of activated sludge has never been reported before.

This study aims to gain insight into the potential acute effects of suspended AlN NPs on SMP of activated sludge. Cultured activated sludge in parallel loaded with 1, 10, 50, 100, 150 and 200 mg/L of AlN NPs was applied to correctly and obviously present results, though the average concentration of NPs was reported at μg/L level in WWTP (Kiser et al., 2010). This study mainly focused on the variation of the constituent, MW and chelation of SMP by various methods, including three-dimensional excitation–emission matrix (EEM) fluorescence spectroscopy, gel filtration chromatography (GFC), *etc.* The dehydrogenase release and oxygen uptake rate (OUR) of activated sludge were also measured for the analysis of bacterial viability.

1. Materials and methods

1.1. AlN NPs preparation

Commercial AlN NPs were purchased from Aladdin (A109771, Shanghai, China) in this study. The transmission electron microscopy (TEM) image of AlN NPs structure was shown in Fig. 1. The primary size of AlN NPs in stock suspension was approximately in the range of 40–60 nm. The AlN NPs stock suspension (10 g/L) was prepared by adding 1 g of AlN NPs to 100 mL of Milli-Q water, followed by 1 hr ultrasonication (25°C, 300 W, 40 kHz) according to the literature (Zheng et al., 2012).

1.2. Activated sludge and media

The inoculating activated sludge was drawn from the return activated sludge stream in the Quyang WWTP. Then the activated sludge was initially operated in a submerged membrane bioreactor (2 L, with the below medium as the influent) for 120 days to achieve steady state for the acclimatization. Before batch experiments, the activated sludge from membrane bioreactor was washed with PBS (NaCl 137 mmol/L, KCl 2.7 mmol/L, Na_2HPO_4 10 mmol/L, KH_2PO_4 2 mmol/L, pH 7.2) for 5 times to remove impurities and Al ions, and re-suspended to the original volume with the below medium.

The medium was synthetized with Mini-Q water according to papers, containing 420 mg/L glucose, 420 mg/L corn starch, 102.75 mg/L NH_4Cl, 28 mg/L peptone, 22 mg/L KH_2PO_4, 9 mg/L $MgSO_4{\cdot}7H_2O$, 3.66 mg/L $MnSO_4{\cdot}H_2O$, 0.55 mg/L $FeSO_4{\cdot}7H_2O$ and 8 mg/L $CaCl_2$. $NaHCO_3$ with a concentration of 120 mg/L was used to maintain the pH at 7.3.

1.3. Batch experiments for potential acute effects of AlN NPs on activated sludge

A series of batch experiments were carried out to identify potential acute effects of AlN NPs on activated sludge. 150 mL pre-treated activated sludge and 50 mL medium were mixed in a 500 mL conical flask. Then conical flasks were added with AlN NPs stock suspension, and the final AlN NPs concentration in each flask was 0 mg/L (blank), 1 mg/L, 10 mg/L, 50 mg/L, 100 mg/L, 150 mg/L, 200 mg/L, respectively. Before all the measurements, the activated sludge, characterized by a final mixed liquor suspended solid (MLSS) of 6.8 g/L and a final mixed liquor volatile suspended solids (MLVSS) of 5.2 g/L, were cultured for 24 hr at 150 r/min and 25°C.

1.4. Viability evaluation of activated sludge

The viability of activated sludge was evaluated by OUR and dehydrogenase activity in this study. OUR was analyzed according to Surmacz-Gorska et al. (1996). Dehydrogenase activity was measured based on a modified method proposed by Zheng et al. (2012). Activated sludge (1 mL), Tris (hydroxymethyl) aminomethane hydrochloride (Tris–HCl) buffer (1.5 mL), 0.4% TTC solution (2 mL) and 0.36% Na_2SO_3 solution (0.5 mL) were sequentially added into 10 mL centrifugal tube. The sample was cultured in the water at 37°C for 20 min. Then 1 mL 37%

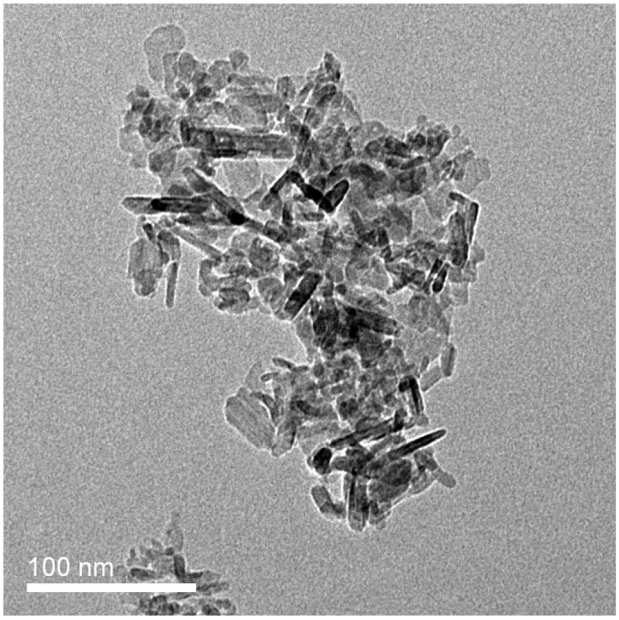

Fig. 1 – The transmission electron microscopy (TEM) image of suspension aluminum nitride nanoparticles (AlN NPs).

formaldehyde was added into sample to end the enzymatic reaction. The sample was centrifuged for 15 min at 4000 r/min to remove the supernatant. The residual sludge was extracted for 10 min with 5 mL 85% acetone. The absorbance of the extracted liquor was measured at 485 nm by a UV–VIS spectrophotometer (4802 UV/VIS, UNICO, USA). The value of dehydrogenase can be calculated according to Eq. (1).

$$\text{Dehydrogenase} = \frac{D_{485}V}{k_T W t} \quad (1)$$

where D_{485} was the absorbance of the supernatant liquor at 485 nm, V (mL) was the volume of extractant, k_T was the slope of calibration curve, W (g) was the dry weight of activated sludge, and t (hr) was the reaction time.

1.5. SMP extraction and measurement

Extraction of SMP was modified according to the method by Xie et al. (2013) from activated sludge. Forty milliliter mixed liquor of activated sludge was first centrifuged (MILTIFUGE X1R, Thermo Electron Corporation, USA) in a 50 mL tube at 6000 g for 5 min. The extracted supernatant was filtrated through a 0.45 μm filter to get SMP.

SMP was normalized as the sum of TOC (total organic carbon), polysaccharide and protein, which were analyzed using a TOC analyzer (TOC-VPN, Shimadzu, Japan), phenol-sulfuric acid method and Coomassie G-250 method, respectively. Because organic compound contains element C, TOC was used to measure semiquantitatively total organic compound in SMP. UV_{254nm} was measured by a UV–VIS spectrophotometer (4802 UV/VIS, UNICO, USA) to represent the humic substances in SMP. Detailed molecular weight distribution and characterization of SMP was measured by a gel filtration chromatography (GFC) analyzer. The GFC system consisted of a TSK G4000SW type gel column (TOSOH Corporation, Japan) and a liquid chromatography spectrometer (LC-10ATVP, SHIMADZU, Japan). Polyethylene glycols (PEGs) with molecular weights (MW) of 1,215,000 Da, 124,700 Da, 11,840 Da, and 620 Da (Merck Corporation, Germany) were used as standards for calibration. The elution at different time intervals was collected by automatic fraction collector and automatically analyzed by using a UV spectroscopy and a dissolved organic carbon (DOC) analyzer to obtain a MW distribution curve. The three-dimensional EEM spectra of biopolymers in cake layer were measured *via* a fluorescence spectrophotometer (FluoroMax-4, HORIBA, Japan). The biopolymers were removed from similar area of the cake layer for both reactors, and dissolved in 5 mL Milli-Q water by 10 min ultrasonication. Then the biopolymers were filtered through a 0.45 μm filter (SCAA-101, ANPEL, China). The EEM spectra were measured with the scanning emission spectra from 200 nm to 550 nm at 5 nm increments by varying the excitation wavelengths from 200 nm to 500 nm at 5 nm sampling intervals.

1.6. Additional analytical methods

MLSS and MLVSS were conducted in accordance with the Standard Methods (APHA, 1998). Concentration of AlN NPs was analyzed *via* an inductively coupled plasma–optical emission spectrometer (ICP–OES, Optima 2100 DV, Perkin Elmer, USA). Dissolved oxygen (DO) concentration and pH were detected by a DO/pH meter (HQ40d, HACH, USA).

1.7. Statistical analysis

Person's product momentum correlation coefficient (r_p, Eq. (2)) was applied for the linear correlation between two parameters.

$$r_p = \frac{\sum\left(x - x_{avg}\right)\left(y - y_{avg}\right)}{\sqrt{\sum\left(x - x_{avg}\right)^2\left(y - y_{avg}\right)^2}} \quad (2)$$

where, (x,y) is a sample of paired data, and x_{avg} and y_{avg} are mean values. Generally, the value of r_p oscillate between −1 and +1, as $r_p = -1$ or $r_p = +1$ represents a perfect correlation, and 0 showed no correction. If $-0.4 < r_p < +0.4$, the correction could be assumed weak and ignored. The positive r_p showed a direct proportionality, while the negative r_p showed an inverse proportionality.

2. Results and discussion

2.1. Potential acute effects of AlN NPs on activated sludge viability

In the batch experiments, MLVSS had no obvious variation ($MLVSS_{beginning}$ = 5.2 ± 0.8 g/L; $MLVSS_{end}$ = 5.0 ± 0.5 g/L) and the MLVSS/MLSS ratio steadied at the range of 76.4–74.2%, indicating that AlN NPs addition had no obvious acute effects on the bacterial amount of activated sludge. As an intracellular enzyme, dehydrogenase and its activity were considered as the useful determination for assessing the toxicity of

various chemicals or wastewater towards bacteria, including activated sludge (Liwarska-Bizukojc, 2011). The high correlation between dehydrogenase and AlN NPs addition (Fig. 2) indicated that AlN NPs addition led to the reduction of dehydrogenase released from the activated sludge. Additionally, dehydrogenase, including aldehyde dehydrogenase, acetaldehyde dehydrogenase, alcohol dehydrogenase, *etc.*, is an enzyme for substrate oxidation by a reduction which transfers on or more hydrides to an electron acceptor. The dehydrogenase activity plays a significant role in the bacterial energy generation cycle system (Appendix A Fig. S1). Consequently, the dehydrogenase decrease with AlN NPs advance predicted that AlN NPs inhibited the bacterial energy supply system and further restrained most of the cell behaviors. Additionally, OUR is applied for the characterization of aerobic bioactivity during the degradation of the organic substrate. The liner correlation between OUR and AlN NPs concentration ($OUR = 8.1–0.02Con._{AlN\ NPs}$) indicated that AlN NPs reduced the respirometric activity of biomass. Respirometric activity represented most of the metabolic pathways for the substrate utilization. OUR result further predicted that AlN NPs led to the inhibition of the substrate utilization and bacterial behaviors. In addition, $r_{p(dehydrogenase\text{-}AlN\ NPs\ concentration)}$ (−0.97) and $r_{p(OUR\text{-}AlN\ NPs\ concentration)}$ (−0.98) also showed that AlN NPs had a highly inverse proportionality to bacterial dehydrogenase and OUR, indicating that AlN NPs had a direct toxicity to the activated sludge viability.

2.2. Fate of AlN NPs in activated sludge

AlN NPs experiments of 1, 10 and 200 mg/L were carried out to investigate the fate of AlN NPs in activated sludge. Fig. 3 showed that about 1% of AlN NPs (AlN NPs was the only Al source in this experiment) were changed into Al ions in the mixed liquid. This was because AlN NPs had a hexagonal crystal structure and was a covalent bonded material. Based on previous studies (Kiser et al., 2010; Lubick, 2008), the NP toxicity was due to the ions released from NPs and the nano-scale. Some studies (Boenigk et al., 2014; Hachicho et al., 2014; Wijnhoven et al., 2009) showed that toxic effects of nano silver were proportional to the activity of free silver ions released by the NPs. In contrast, NPs could cause the release of H_2O_2, leading to higher toxicity than their macroscopic counterparts (Batchelor-McAuley et al., 2014; Choi and Hu, 2008; Guo et al., 2013). In this study, AlN NPs did not release much Al ions into mixed liquid in 24 hr, predicting that the toxicity of AlN NPs should be due to NP scale, not the Al ions released from AlN NPs.

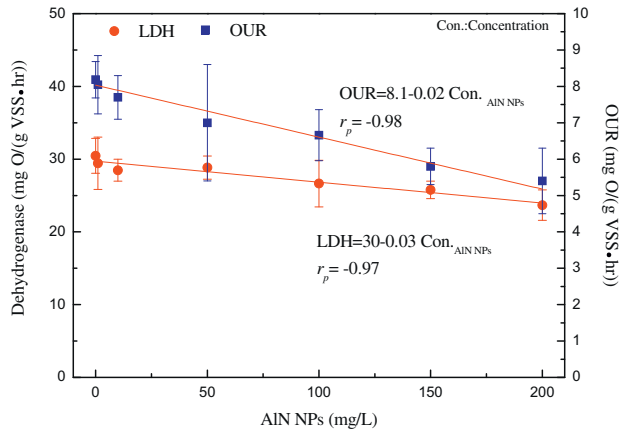

Fig. 2 – Variations of dehydrogenase and oxygen uptake rate (OUR) in activated sludge (n = 3).

In Appendix A Fig. S2, crystal particles were found on the bacterial cell surface. EDX also identified that the crystal particles contained Al element. AlN NPs was the only Al source in this study, indicating that AlN NPs partly attached to the bacteria surface. Previous studies (Lee et al., 2011, 2015; Nel et al., 2006) also showed that NP easily attached to the cell surface. Consequently, AlN NPs mainly distributed in the mixed liquid and bacteria surface in the form of nano-scale.

2.3. Potential acute effects of AlN NPs on SMP of activated sludge

2.3.1. Constituent of SMP

SMP has a complex constituent, including polysaccharide, proteins, humic and fulvic acids, nucleic acids, organic acids, amino acids, antibiotics, exocellular enzymes, *etc.* (Xie et al., 2013). Protein and TOC only had slight variations along with the AlN NPs addition (Table 1). Additionally, the $r_{p(protein\text{-}AlN\ NPs\ concentration)}$ were only −0.12, indicating that AlN NPs had no obvious influences on the protein release of bacteria. Therefore, AlN NPs had the slight, but not obvious toxicity to bacteria. It was evident that the toxicity of NP was mainly due to its nano-scale and/or its releasing ions. The protein structure was tightly maintained with the shape complementarity of the hydrophobic residues. However, the govern the protein structure were counterbalanced by a large entropy loss associated with going from a large ensemble of states to a more restricted set of conformations, and the repulsive electrostatic interactions (Kumar and Nussinov, 2001). Thus NP could easily disrupt the protein structure and form the floc structure by the interaction with protein surface due to the nano-scale (Lynch and Dawson, 2008). In other NP toxicity studies, nano silver leading to protein decrease was due to that the Ag ions inhibited cellular respiration and transport of ions across membranes (Fabrega et al., 2011; Luoma, 2008). But Al_{n+} remained at 0.01 mg/L in all experiments during the first 24 hr, indicating that the toxicity of AlN NP should not be because of the releasing ion. Consequently, the slight but not obvious toxicity of AlN to protein was due to its nano-scale. On the contrary, polysaccharide and UV_{254nm} (showing humic substances) presented obvious decrease with the AlN NPs addition ($r_{p(polysaccharide\text{-}\ –\ AlN\ NPs\ concentration)} = −0.68$; $r_{p(UV254\ nm\text{-}\ –\ AlN\ NPs\ concentration)} = −0.43$ (Table 1)). According to Philippe and Schaumann (2014), organic compounds, especially polysaccharide (0.18–3000 kDa) and humic compounds (2–5 kDa) (protein is normally in the range of 10–a few 1000), had the high affinity to be adsorbed onto the NP surface due to the nano-scale. Additionally, Philippe and Schaumann (2014) also reviewed that aluminous NP was easily adsorbed on the surface of polysaccharide and humic compounds due to van der Waals and hydrophobic forces, as well as the carboxyl and hydroxyl groups. Therefore, the nano-scale of AlN NPs obviously easily adsorbed to the surface of the polysaccharide and humic

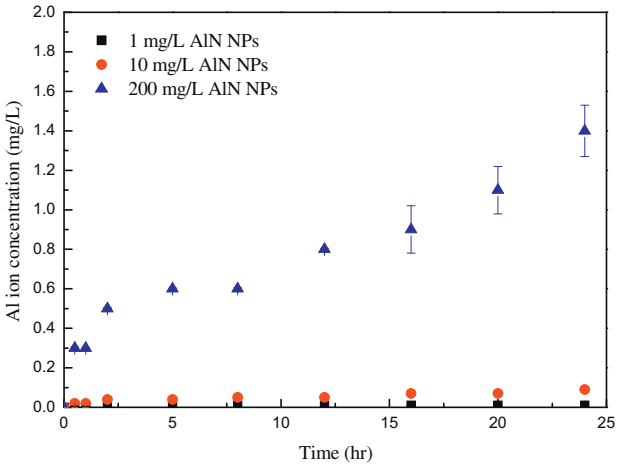

Fig. 3 – Al ion concentration in the mixed liquor during the experiment (n = 3).

compounds, leading to the polysaccharide and humic compounds decrease.

2.3.2. Fluorescence characteristics of SMP

Fluorescent peak A (Fig. 4a–g) was found in the three-dimensional EEM fluorescence spectra of SMP. Peak A was at the excitation/emission wavelengths (Ex/Em) of 270–285/320–330 nm, which had been reported as tryptophan-like substances (Xia et al., 2015). The fluorescence intensity (FI) of the spectra could be used for quantitative analyses. As Fig. 4h showed, tryptophan-like substances (Peak A) decreased obviously with AlN NPs advance and $r_{p(\text{Peak A FI-AlN NPs concentration})}$ was −0.92, predicting a highly inverse proportionality between tryptophan-like substances and AlN NPs. Tryptophan-like substances, containing α-amino group, an α-carboxylic acid group, and a side chain indole (Appendix A Fig. S3), was an α-amino acid used in the biosynthesis of proteins. Tryptophan-like substances played the important role in the bacterial metabolism and protection system, and acted as building blocks in protein biosynthesis (Schröcksnadel et al., 2006; Xia et al., 2015). Consequently, tryptophan-like substances decrease predicted that bacterial protection function dropped down, indicating the direct toxicity of AlN NPs to the activated sludge viability, which was inconsistent with the result of Section 2.1. Additionally, as Yang et al. (2009) reported, –OH and –COOH would easily attach onto NP surface due to the nano-scale (Fig. S4). Philippe and Schaumann (2014) and Lynch and Dawson (2008) both showed that NP could easily disturb protein structure and adsorb onto protein surface by the combination with –OH and –COOH. Kaur et al. (2013) indicated that nano-scale could enhance the absorption of NP to tryptophan-like substances. Therefore, the tryptophan-like substances decrease was mainly due to the absorption of AlN NPs onto the –COOH of tryptophan-like substance surface, and further the nano-scale could enhance the absorption process.

Table 1 – Variations of protein, polysaccharide, TOC and UV_{254nm} with AlN NPs addition. (n = 3).

AlN NPs Con.[a]	Protein[b]	Polysaccharide[b]	TOC[b]	UV_{254nm}[c]
0 mg/L	14.0 ± 0.10	56.65 ± 0.50	67.95 ± 0.12	0.211 ± 0.003
1 mg/L	13.1 ± 0.12	52.22 ± 0.64	69.51 ± 0.23	0.209 ± 0.004
10 mg/L	13.5 ± 0.22	53.50 ± 0.20	66.51 ± 0.12	0.231 ± 0.0001
50 mg/L	13.0 ± 0.14	47.07 ± 0.15	70.23 ± 0.33	0.212 ± 0.006
100 mg/L	13.2 ± 0.11	51.08 ± 0.32	66.09 ± 0.12	0.221 ± 0.003
150 mg/L	13.3 ± 0.40	46.61 ± 0.11	69.51 ± 0.41	0.201 ± 0.004
200 mg/L	13.5 ± 0.20	48.88 ± 0.12	65.55 ± 0.21	0.208 ± 0.002
r_p[d]	−0.12	−0.68	−0.34	−0.43

TOC: total organic carbon; AlN NPs: aluminum nitride nanoparticles; MLVSS: mixed liquor volatile suspended solids; SMP: soluble microbial products; UV: ultraviolet.
[a] Con.: concentration.
[b] mg/g MLVSS.
[c] No unit.
[d] r_p between each constituent in SMP and AlN NPs concentration; no unit.

2.3.3. MW distribution of SMP

Since the concentration of total SMP is changed, MW distribution (size-fractionated) of SMP would not be normally considered to be the study item. However, membrane technology has been applied wildly in wastewater treatment in recent 20 years, and MW distribution of SMP has been considered as the significant factor on membrane fouling (Zhang et al., 2015, 2016). Based on previous study (Arabi and Nakhla, 2010), MW distribution of SMP is classed into four critical MW range: >100 kDa, 10–100 kDa, 1–10 kDa and <1 kDa. The MW distributions of SMP with different concentration AlN NPs addition were summarized in Table 2. The SMP compounds had a broad MW distribution, which was ranging from low MW (<1 kDa) to a large size (>100 kDa). The SMP in the range of 1–10 kDa increased with AlN NPs addition, but SMP ranging >100 kDa and 10–100 kDa decreased with the AlN NPs advance. As the majority substances of SMP, MWs of protein, polysaccharide and humic acid were in the range of 10-a few 1000 kDa, 0.18–3000 kDa and 2–5 kDa, respectively (Philippe and Schaumann, 2014), indicating that SMP in the range of 10–100 kDa and >100 kDa were mainly protein and polysaccharide. As Table 1 showed, the decrease of 10–100 kDa and >100 kDa substances in SMP were due to the amount decrease of protein and polysaccharide. The high ionic strength in the medium inhibited NP self-aggregation and also reduced the electrostatic stabilization due to charge screening, enhancing the chelation with organic matters (Louie et al., 2013). Additionally, Aiken et al. (2011) reported that engineered NP chelated to the functional groups and metal on the surface of organic matters, and transformed into colloid. Yin et al. (2015) also showed that organic matter with high MW (>100 kDa and 30–100 kDa) promoted the aggregation of NP in mono- and divalent electrolyte solution, but organic matter ranging <30 kDa inhibited the aggregation process, indicating that SMP in the range of >30 kDa would aggregated with NP and formed into colloid. Therefore, the decrease of 10–100 kDa and >100 kDa substances in SMP with AlN NPs addition

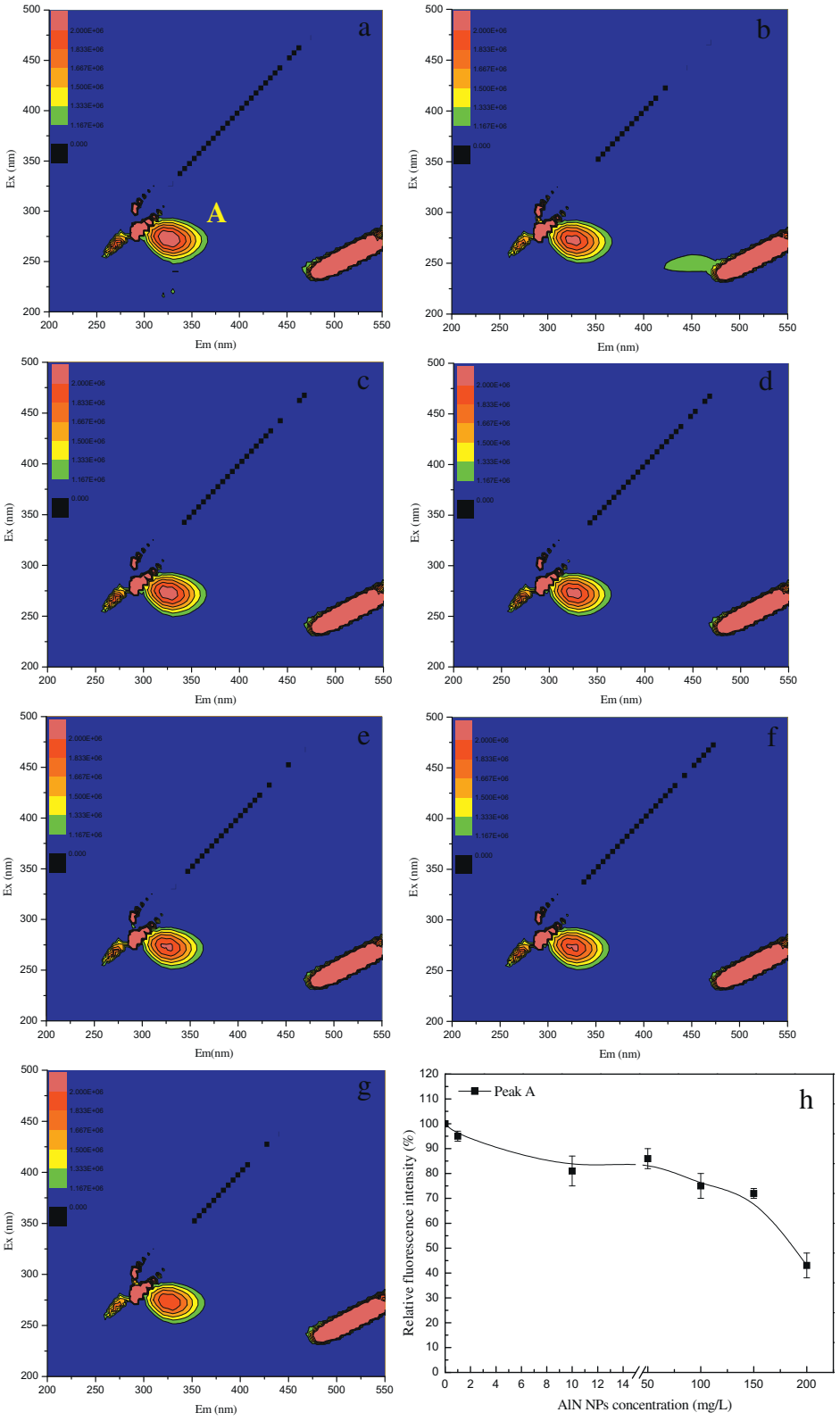

Fig. 4 – EEM fluorescence spectra of SMP with (a) 0 mg/L, (b) 1 mg/L, (c) 10 mg/L, (d) 50 mg/L, (e) 100 mg/L, (f) 150 mg/L, (g) 200 mg/L AlN NPs. (h) The relative fluorescence intensity variations of Peak A with the AlN NPs increase (n = 3).

were mainly due to the aggregation with NP. In addition, Arabi and Nakhla (2010) reported that SMP in the range of >100 kDa and 1–10 kDa had no obvious correlation with membrane fouling, but SMP ranging 10–100 kDa played the significant role in membrane fouling and had been proved as the most important fraction from a fouling perspective. Consequently,

Table 2 – Percentage of each MW range compound in SMP with AlN NPs addition (n = 3).

	<1 kDa	1–10 kDa	10–100 kDa	>100 kDa
0 mg AlN NPs/L	0.05% ± 0.01%	0.02% ± 0.03%	71.47% ± 2.45%	28.46% ± 1.56%
1 mg AlN NPs/L	0.09% ± 0.01%	5.19% ± 0.60%	71.26% ± 3.14%	23.46% ± 4.13%
10 mg AlN NPs/L	0.08% ± 0.01%	11.74% ± 0.82%	65.59% ± 3.57%	22.59% ± 1.45%
50 mg AlN NPs/L	0.07% ± 0.02%	20.13% ± 2.43%	59.34% ± 3.41%	20.46% ± 4.41%
100 mg AlN NPs/L	0.08% ± 0.01%	21.24% ± 1.84%	58.72% ± 1.43%	19.96% ± 2.45%
150 mg AlN NPs/L	0.08% ± 0.01%	28.40% ± 2.01%	53.07% ± 3.53%	18.45% ± 1.53%
200 mg AlN NPs/L	0.12% ± 0.02%	31.96% ± 1.21%	50.88% ± 2.41%	17.04% ± 2.41%

AlN NPs should mitigate membrane fouling process due to the 10–100 kDa SMP decrease with AlN NPs addition.

In order to better understand potential acute effects of AlN NPs on the MW distributions of SMP, the evaluations of number-average molecular weight (Mn) were employed in Fig. 5. The Mn of SMP decreased with the AlN NPs advance, and $r_{p(\text{Mn-AlN NPs concentration})}$ was −0.97, indicating the highly inverse proportionality of AlN NPs to the MW of SMP. In previous researches (Lee et al., 2011; Liu et al., 2016; Xia et al., 2015), bacteria would release low MW proteins through its immunity system with toxicity shock, then leading to MW decrease. Yin et al. (2015) also predicted that NP chelated with high MW organic matter, and left the low MW organic matter in the aqua. Consequently, AlN NPs addition could lead obviously to the Mn decrease of SMP.

3. Conclusion

Potential acute effects of suspended AlN NPs on SMP of activated sludge were studied. AlN NPs had the direct toxicity to the activated sludge viability, which was mainly due to the nano-scale of AlN NPs. In SMP, AlN NPs caused the decrease of polysaccharide and humic compounds, but had no obvious effects on protein. The decrease of tryptophan-like substances in SMP indicated the inhibition of AlN NPs on the bacterial metabolism. Additionally, AlN NPs reduced obviously the MW of SMP, which might be due to the nano-scale of AlN.

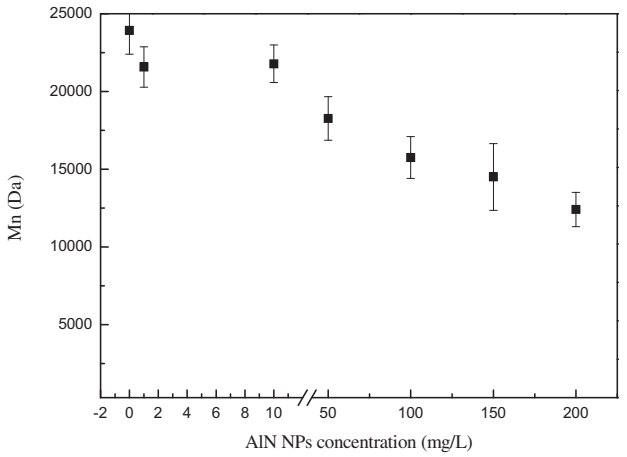

Fig. 5 – Mn variations of SMP in activated sludge with different concentration AlN NPs addition (n = 3).

Acknowledgements

This work was supported by the National Natural Science Foundation of China (No. 51378368), the Foundation of State Key Laboratory of Pollution Control and Resource Reuse (Tongji University), China (No. PCRRT16003) and Shenzhen Science and Technology Research Fund (No. CXZZ20150330151321966).

Appendix A. Supplementary data

Supplementary data to this article can be found online at http://dx.doi.org/10.1016/j.jes.2017.02.001.

REFERENCES

Aiken, G.R., Hsu-Kim, H., Ryan, J.N., 2011. Influence of dissolved organic matter on the environmental fate of metals, nanoparticles, and colloids. Environ. Sci. Technol. 45, 3196–3201.

APHA, 1998. Standard Methods for the Examination of Water and Wastewater. 20th ed. American Pubilc Health Association, Washington, DC, USA.

Arabi, S., Nakhla, G., 2010. Impact of molecular weight distribution of soluble microbial products on fouling in membrane bioreactors. Sep. Purif. Technol. 73, 391–396.

Aslam, M., Charfi, A., Lesage, G., Heran, M., Kim, J., 2017. Membrane bioreactors for wastewater treatment: a review of mechanical cleaning by scouring agents to control membrane fouling. Chem. Eng. J. 307, 897–913.

Batchelor-McAuley, C., Tschulik, K., Neumann, C., Laborda, E., Compton, R.G., 2014. Why are silver nanoparticles more toxic than bulk silver? Towards understanding the dissolution and toxicity of silver nanoparticles. Int. J. Electrochem. Sci. 9, 1132–1138.

Boenigk, J., Beisser, D., Zimmermann, S., Bock, C., Jakobi, J., Grabner, D., Groβmann, L., Rahmann, S., Barcikowski, S., Sures, B., 2014. Effects of silver nitrate and silver nanoparticles on a planktonic community: general trends after short-term exposure. PLoS One 9, e95340.

Campo, R., Di Prima, N., Freni, G., Giustra, M.G., Di Bella, G., 2016. Start-up of two moving bed membrane bioreactors treating saline wastewater contaminated by hydrocarbons. Water Sci. Technol. 73, 716–724.

Campo, R., Capodici, M., Di Bella, G., Torregrossa, M., 2017. The role of EPS in the foaming and fouling for a MBR operated in intermittent aeration conditions. Biochem. Eng. J. 118, 41–52.

Choi, O., Hu, Z., 2008. Size dependent and reactive oxygen species related nanosilver toxicity to nitrifying bacteria. Environ. Sci. Technol. 42, 4583–4588.

Deng, L.J., Guo, W.S., Ngo, H.H., Zhang, H.W., Wang, J., Li, J.X., Xia, S.Q., Wu, Y., 2016. Biofouling and control approaches in membrane bioreactors. Bioresour. Technol. 221, 656–665.

Fabrega, J., Luoma, S.N., Tyler, C.R., Galloway, T.S., Lead, J.R., 2011. Silver nanoparticles: behaviour and effects in the aquatic environment. Environ. Int. 37, 517–531.

Guo, D., Bi, H., Liu, B., Wu, Q., Wang, D., Cui, Y., 2013. Reactive oxygen species-induced cytotoxic effects of zinc oxide nanoparticles in rat retinal ganglion cells. Toxicol. in Vitro 27, 731–738.

Hachicho, N., Hoffmann, P., Ahlert, K., Heipieper, H.J., 2014. Effect of silver nanoparticles and silver ions on growth and adaptive response mechanisms of Pseudomonas putida mt-2. FEMS Microbiol. Lett. 355, 71–77.

Holakoo, L., Nakhla, G., Yanful, E.K., Bassi, A.S., 2006. Chelating properties and molecular weight distribution of soluble microbial products from an aerobic membrane bioreactor. Water Res. 40, 1531–1538.

Jo, S.J., Kwon, H., Jeong, S.Y., Lee, S.H., Oh, H.S., Yi, T., Lee, C.H., Kim, T.G., 2016. Effects of quorum quenching on the microbial community of Biofilm in an anoxic/oxic MBR for wastewater treatment. J. Microbiol. Biotechnol. 26, 1593–1604.

Kaur, B., Pandiyan, T., Satpati, B., Srivastava, R., 2013. Simultaneous and sensitive determination of ascorbic acid, dopamine, uric acid, and tryptophan with silver nanoparticles-decorated reduced graphene oxide modified electrode. Colloids Surf. B. Biointerfaces 111, 97–106.

Kiser, M.A., Westerhoff, P., Benn, T., Wang, Y., Perez-Rivera, J., Hristovski, K., 2009. Titanium nanomaterial removal and release from wastewater treatment plants. Environ. Sci. Technol. 43, 6757–6763.

Kiser, M.A., Ryu, H., Jang, H.Y., Hristovski, K., Westerhoff, P., 2010. Biosorption of nanoparticles to heterotrophic wastewater biomass. Water Res. 44, 4105–4114.

Kumar, S., Nussinov, R., 2001. How do thermophilic proteins deal with heat? Cell. Mol. Life Sci. 58, 1216–1233.

Kunacheva, C., Stuckey, D.C., 2014. Analytical methods for soluble microbial products (SMP) and extracellular polymers (ECP) in wastewater treatment systems: a review. Water Res. 61, 1–18.

Lee, S., Kim, K., Shon, H.K., Kim, S.D., Cho, J., 2011. Biotoxicity of nanoparticles: effect of natural organic matter. J. Nanopart. Res. 13, 3051–3061.

Lee, Y.C., Lee, K., Oh, Y.K., 2015. Recent nanoparticle engineering advances in microalgal cultivation and harvesting processes of biodiesel production: a review. Bioresour. Technol. 184, 63–72.

Lerner, M.I., Lozhkomoev, A.S., Pervikov, A.V., Bakina, O.V., 2016. Synthesis of Al-Al_2O_3 and Al-Aln nanoparticle composites via electric explosion of wires. Russ. Phys. J. 59, 422–429.

Lin, H.J., Zhang, M.J., Wang, F.Y., Meng, F.G., Liao, B.Q., Hong, H.C., Chen, J.R., Gao, W.J., 2014. A critical review of extracellular polymeric substances (EPSs) in membrane bioreactors: characteristics, roles in membrane fouling and control strategies. J. Membr. Sci. 460, 110–125.

Liu, J., Feng, X., Wei, L., Chen, L., Song, B., Shao, L., 2016. The toxicology of ion-shedding zinc oxide nanoparticles. Crit. Rev. Toxicol. 46, 348–384.

Liwarska-Bizukojc, E., 2011. Influence of Imidazolium ionic liquids on dehydrogenase activity of activated sludge microorganisms. Water Air Soil Pollut. 221, 327–335.

Louie, S.M., Tilton, R.D., Lowry, G.V., 2013. Effects of molecular weight distribution and chemical properties of natural organic matter on gold nanoparticle aggregation. Environ. Sci. Technol. 47, 4245–4254.

Lubick, N., 2008. Nanosilver toxicity: ions, nanoparticles-or both? Environ. Sci. Technol. 42, 8617-8617.

Luoma, S.N., 2008. Silver Nanotechnologies and the Environment. Woodrow Wilson International Center for Scholars, Washington, DC, USA, p. 72.

Lynch, I., Dawson, K.A., 2008. Protein-nanoparticle interactions. Nano Today 3, 40–47.

Ma, Z., Yin, X.Y., Ji, X.S., Yue, J.Q., Zhang, L.F., Qin, J.J., Valiyaveettil, S., Adin, A., 2016. Evaluation and removal of emerging nanoparticle contaminants in water treatment: a review. Desalin. Water Treat. 57, 11221–11232.

Nel, A., Xia, T., Madler, L., Li, N., 2006. Toxic potential of materials at the nanolevel. Science 311, 622–627.

Ni, B.J., Yu, H.Q., 2012. Microbial products of activated sludge in biological wastewater treatment systems: a critical review. Crit. Rev. Environ. Sci. Technol. 42, 187–223.

Philippe, A., Schaumann, G.E., 2014. Interactions of dissolved organic matter with natural and engineered inorganic colloids: a review. Environ. Sci. Technol. 48, 8946–8962.

Schröcksnadel, K., Wirleitner, B., Winkler, C., Fuchs, D., 2006. Monitoring tryptophan metabolism in chronic immune activation. Clin. Chim. Acta 364, 82–90.

Shaalan, M., Saleh, M., El-Mahdy, M., El-Matbouli, M., 2016. Recent progress in applications of nanoparticles in fish medicine: a review. Nanomed. Nanotechnol. Biol. Med. 12, 701–710.

Shen, Y.X., Zhao, W.T., Xiao, K., Huang, X., 2010. A systematic insight into fouling propensity of soluble microbial products in membrane bioreactors based on hydrophobic interaction and size exclusion. J. Membr. Sci. 346, 187–193.

Shen, Y.X., Xiao, K., Liang, P., Sun, J.Y., Sai, S.J., Huang, X., 2012. Characterization of soluble microbial products in 10 large-scale membrane bioreactors for municipal wastewater treatment in China. J. Membr. Sci. 415, 336–345.

Surmacz-Gorska, J., Gernaey, K., Demuynck, C., Vanrolleghem, P., Verstraete, W., 1996. Nitrification monitoring in activated sludge by oxygen uptake rate (OUR) measurements. Water Res. 30, 1228–1236.

Vale, G., Mehennaoui, K., Cambier, S., Libralato, G., Jomini, S., Domingos, R.F., 2016. Manufactured nanoparticles in the aquatic environment-biochemical responses on freshwater organisms: a critical overview. Aquat. Toxicol. 170, 162–174.

Wang, Q.Y., Wang, Z.W., Zhu, C.W., Mei, X.J., Wu, Z.C., 2013. Assessment of SMP fouling by foulant-membrane interaction energy analysis. J. Membr. Sci. 446, 154–163.

Wijnhoven, S.W., Peijnenburg, W.J., Herberts, C.A., Hagens, W.I., Oomen, A.G., Heugens, E.H., Roszek, B., Bisschops, J., Gosens, I., Van De Meent, D., 2009. Nano-silver-a review of available data and knowledge gaps in human and environmental risk assessment. Nanotoxicology 3, 109–138.

Xia, S.Q., Zhou, L.J., Zhang, Z.Q., Hermanowicz, S.W., 2015. Removal mechanism of low-concentration Cr (VI) in a submerged membrane bioreactor activated sludge system. Appl. Microbiol. Biotechnol. 99, 5351–5360.

Xie, W.M., Ni, B.J., Seviour, T., Yu, H.Q., 2013. Evaluating the impact of operational parameters on the formation of soluble microbial products (SMP) by activated sludge. Water Res. 47, 1073–1079.

Yang, K., Lin, D., Xing, B., 2009. Interactions of humic acid with nanosized inorganic oxides. Langmuir 25, 3571–3576.

Yin, Y.G., Shen, M.H., Tan, Z.Q., Yu, S.J., Liu, J.F., Jiang, G.B., 2015. Particle coating-dependent interaction of molecular weight fractionated natural organic matter: impacts on the aggregation of silver nanoparticles. Environ. Sci. Technol. 49, 6581–6589.

Zhang, H.F., Wang, B., Yu, H.H., Zhang, L.H., Song, L.F., 2015. Relation between sludge properties and filterability in MBR: under infinite SRT. Membr. Water Treat. 6, 501–512.

Zhang, D.Q., Trzcinski, A.P., Kunacheva, C., Stuckey, D.C., Liu, Y., Tan, S.K., Ng, W.J., 2016. Characterization of soluble microbial products (SMPs) in a membrane bioreactor (MBR) treating synthetic wastewater containing pharmaceutical compounds. Water Res. 102, 594–606.

Zheng, X., Su, Y., Chen, Y., 2012. Acute and chronic responses of activated sludge viability and performance to silica nanoparticles. Environ. Sci. Technol. 46, 7182–7188.

Zhou, Z.B., Meng, F.G., Liang, S., Ni, B.J., Jia, X.S., Li, S.Y., Song, Y.K., Huang, G.C., 2012. Role of microorganism growth phase in the accumulation and characteristics of biomacromolecules (BMM) in a membrane bioreactor. RSC Adv. 2, 453–460.

Zhou, L., Zhang, Z., Xia, S., Jiang, W., Ye, B., Xu, X., Gu, Z., Guo, W., Ngo, H.-H., Meng, X., Fan, J., Zhao, J., 2014. Effects of suspended titanium dioxide nanoparticles on cake layer formation in submerged membrane bioreactor. Bioresour. Technol. 152, 101–106.